24th INTERNATIONAL CONGRESS ON SOUND AND VIBRATION
23–27 July 2017, London

# FLUID-STRUCTURE INTERACTION ANALYSIS OF COCHLEA IN A FINITE ELEMENT MODEL WITH TRANSVERSE ISOTROPIC BASILAR MEMBRANE

Dooho Lee

*Dongeui University, Dept. of Mechanical Engineering, Busan, Republic of Korea*
*email: dooho@deu.ac.kr*

Seong-Jung Kang

*Dongeui University, Dept. of Mechanical Engineering, Busan, Republic of Korea*

In this paper, a finite element (FE) model for the cochlea was developed and used to investigate the vibrational characteristics of basilar membrane. The geometry of cochlea was simplified as a rectangular duct that includes the basilar membrane, osseous spiral lamina, cochlear fluid, and oval and round windows. The basilar membrane was assumed to be transverse isotropic properties with different values along the longitudinal direction. The oval and the round windows were modeled as thin shells with different thicknesses and material properties. The cochlear fluid was assumed to be compressible inviscid and was coupled with all structural elements. Harmonic frequency responses were calculated using commercial software, MSC/NASTRAN with direct frequency analysis method. The fluid-structure interaction model showed that the transverse isotropic characteristics of the basilar membrane resulted in different motions of the basilar membrane near 5 kHz frequency region. It will be discussed whether the difference can explain the noise induced hearing loss on the same frequency region.

Keywords: fluid-structure interaction, finite element model, transverse isotropic basilar membrane

## 1. Introduction

Sound transmitted into ear is coded as dynamic motion of basilar membrane in cochlea of human hearing system, and interpreted as electro-chemical signal in the organ of corti of the cochlea. Thus, the regeneration of basilar membrane motion due to sound stimuli is very important in understanding of the physiology of sound transmission including the detail mechanism of noise-induced hearing loss. A finite element (FE) model for the basilar membrane helps to intuitively understand the complex mechanism of the hearing system because it can show the detail motion for all geometry positions [1, 2].

The basilar membrane is immersed in the fluid-filled ducts, the scala vestibule (SV), the scala tympani, and the scale media(SM). Many researchers have developed fluid-structure interaction models for the cochlea [3-8]. Emadi et al.[9] showed through many measurements that the basilar membrane has orthotropic material properties in stiffness for the gerbil basilar membrane.

In this paper, an FE model for the cochlea is presented. The FE model considers the fluid-structure interaction with the assumption of non-viscous compressible fluid. For the basilar membrane the transversely isotropic material properties are included in the FE model. Using the developed FE

model, the motions of basilar membrane are investigated over 4~6 kHz frequency band and are compared with that of the isotropic basilar membrane model.

## 2. Fluid-structure analysis of cochlea

In this section, the finite element model of the cochlea is described.

### 2.1 Fluid-structure interactions

Perilymph and endolymph surround the basilar membrane, and mutual interactions of the fluid-structure should be considered in finite element analysis. The fluids are assumed as non-viscous compressible fluid. Then the discretized governing equations are as follows.

$$\begin{bmatrix} \boldsymbol{M_s} & \boldsymbol{0} \\ -\boldsymbol{A^T} & \boldsymbol{M_f} \end{bmatrix} \begin{Bmatrix} \ddot{\boldsymbol{u}}_s \\ \ddot{\boldsymbol{p}} \end{Bmatrix} + \begin{bmatrix} \boldsymbol{B_s} & \boldsymbol{0} \\ \boldsymbol{0} & \boldsymbol{B_f} \end{bmatrix} \begin{Bmatrix} \dot{\boldsymbol{u}}_s \\ \dot{\boldsymbol{p}} \end{Bmatrix} + \begin{bmatrix} \boldsymbol{K_s} & \boldsymbol{A} \\ \boldsymbol{0} & \boldsymbol{K_f} \end{bmatrix} \begin{Bmatrix} \boldsymbol{u}_s \\ \boldsymbol{p} \end{Bmatrix} = \begin{Bmatrix} \boldsymbol{P_s} \\ \boldsymbol{P_f} \end{Bmatrix} \quad \textbf{(1)}$$

where $u_s$ refers the displacement of structure, and $p$ the pressure of fluid. $\dot{}$ on an argument refers the time derivative. The matrices$M_s, M_f$ refer the mass matrix of structure and fluid, respectively, and the matrices $B_s, B_f$ refer the damping matrix of structure and fluid, and the matrices $K_s, K_f$ are the stiffness matrix of structure and fluid, respectively. The matrix $A$ refers the structure-fluid coupling matrix. The vectors $P_s$, $P_f$ refer the external loading of structure and fluid, respectively.

### 2.2 Model geometry and discretization

Uncoiling of the spiral cochlea and simplifying the shape of ducts, the finite element model was constructed as shown in Fig. 1.

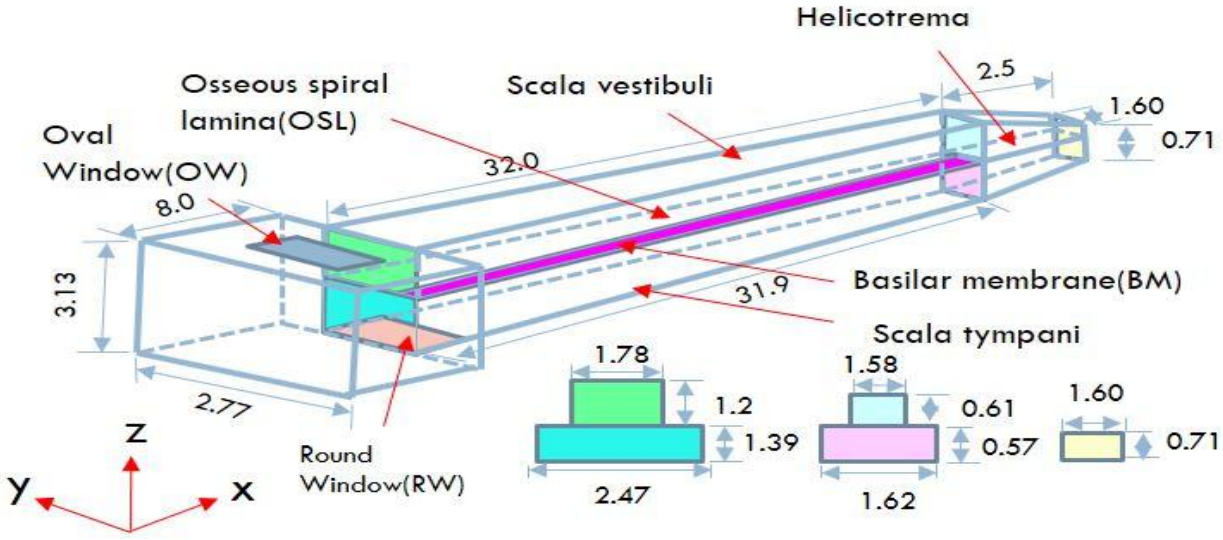


Figure 1: The geometry and components of the cochlea FE model.

In the FE model, the length of basilar membrane was 32 mm. The width and thickness of the basilar membrane vary linearly 0.1 mm, 7.5 μm to 0.5 mm, 3.2 μm, respectively from base to apex along the basilar membrane. The size of the duct was taken from a CT-scanned geometry of a human cochlea[10].

Four-node shell elements discretized the structural parts of the cochlea such as OW, OSL, RW and BM with 7,716 nodes. For the fluid, 336,561 8-node hexahedron solid elements discretized the ducts.

### 2.3 Material properties

The basilar membrane has transverse orthotropic material properties. The stress-strain relation in linear elasticity with the transverse isotropic material is as follows.

$$\begin{bmatrix}\sigma_1\\ \sigma_2\\ \sigma_3\\ \sigma_4\\ \sigma_5\\ \sigma_6\end{bmatrix} = \begin{bmatrix} C_{11} & C_{12} & C_{13} & 0 & 0 & 0 \\ C_{12} & C_{11} & C_{13} & 0 & 0 & 0 \\ C_{13} & C_{13} & C_{33} & 0 & 0 & 0 \\ 0 & 0 & 0 & C_{44} & 0 & 0 \\ 0 & 0 & 0 & 0 & C_{44} & 0 \\ 0 & 0 & 0 & 0 & 0 & (C_{11}-C_{12})/2 \end{bmatrix} \begin{bmatrix}\varepsilon_1\\ \varepsilon_2\\ \varepsilon_3\\ \varepsilon_4\\ \varepsilon_5\\ \varepsilon_6\end{bmatrix} \quad (2)$$

where σ and ε refer the stress and strain, respectively. The stiffness matrix $C_{ij}$ has 5 independent constants. In this study, the isotropy was set to the xz plane in Fig. 1. Figure 2 shows the elastic moduli of the transverse and longitudinal directions. The other isotropic material properties are listed in Tables 1~2.

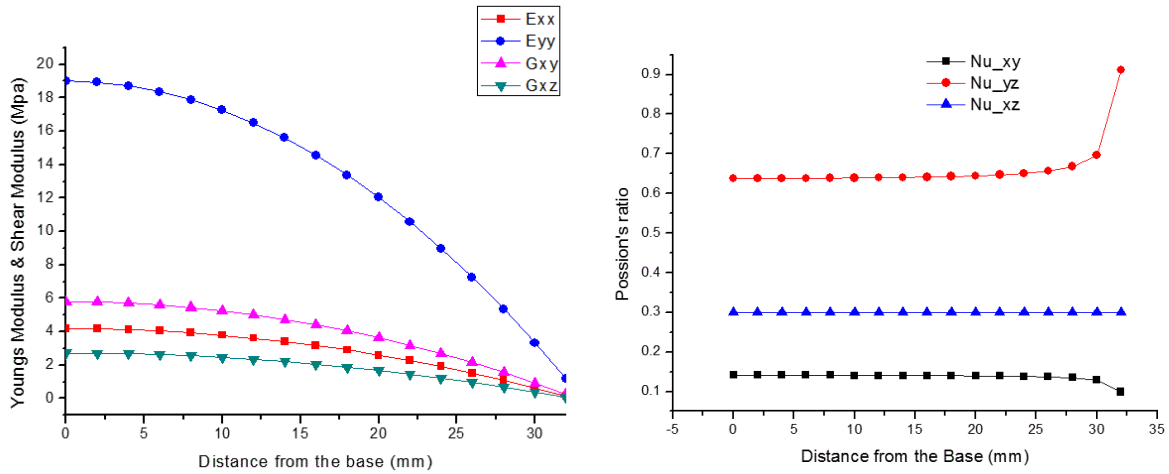


**Fig. 2. Material properties of BM in the cochlear model.**

**Table 1: Material properties of FE model for cochlea**

| Material | Young's modulus | Poisson's ratio | Density ($kg/m^3$) | Loss factor |
|---|---|---|---|---|
| OSL | 200 GPa | 0.3 | 1200 | |
| OW | 5.5 MPa | 0.3 | 1200 | |
| RW | 2.5 MPa | 0.3 | 1200 | |

**Table 2: Fluid properties of FE model for cochlea**

| Material | Bulk modulus | Speed of sound (m/s) | Density ($kg/m^3$) | Loss factor |
|---|---|---|---|---|
| Fluid | 2.2 GPa | 1500 | 1000 | 0.01 |

## 3. Results and Discussions

The FE model described in previous section was used to calculate the motion of the basilar membrane due to unit normal velocity of the oval window using MSC/NASTRAN software[11]. The direct frequency analysis module was used to obtain the harmonic motion of the cochlea.

## 3.1 Cochlear map

The positions of maximum displacement due to the harmonic excitations were summarized as the cochlear map as shown in Fig. 3. In Fig. 3, the results of the FE model was compared with an experimental one[12]. In the Fig. 3, the results of isotropic FE models with different values (4.3 MPa is a typical value for BM) were also plotted for comparison. It is shown in Fig. 3 that the transverse isotropic BM model has the best representation of the measured cochlear map.

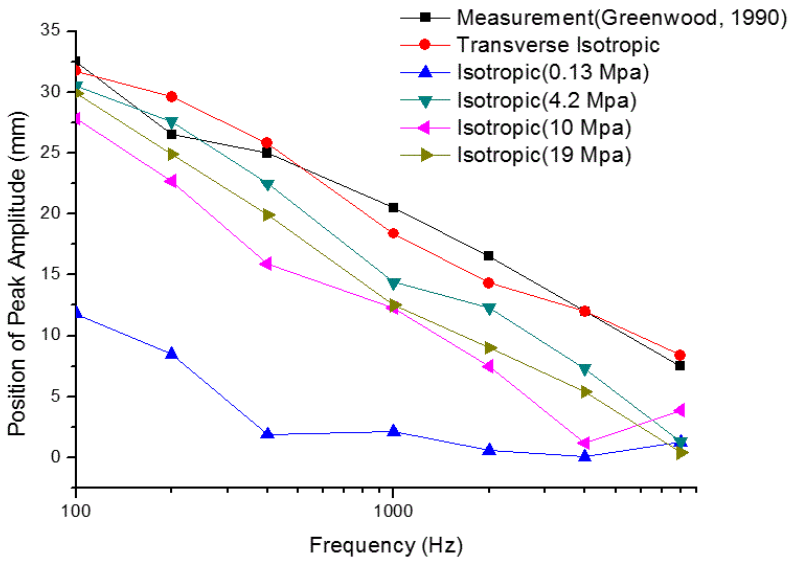


**Fig. 3. Cochlear map of the FE model.**

## 3.2 Response of the BM

The motion of the BM calculated by the transverse isotropic FE model is plotted in Fig. 4. The motions are taken from the nodal displacements of the centre line of the BM. It should be noted in Fig. 4 that the smaller displacements on the higher frequency are originated from the unit velocity excitation. Figure 4 well illustrates the frequency characteristic of the BM motion: i.e., the position of maximum displacement moves to the base from the apex according to the higher excitation frequency.

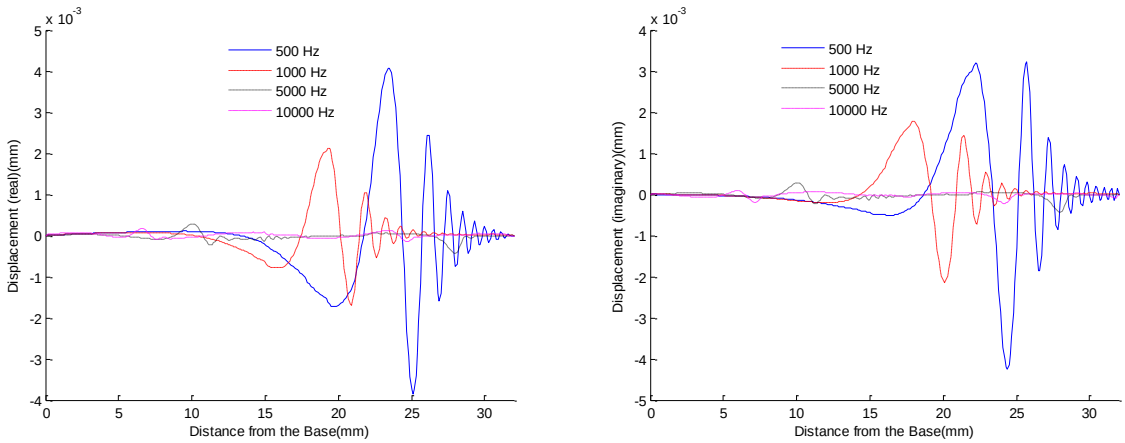


**Fig. 4. Motions of the BM due to unit velocity on the OW in the transverse isotropic FE model**

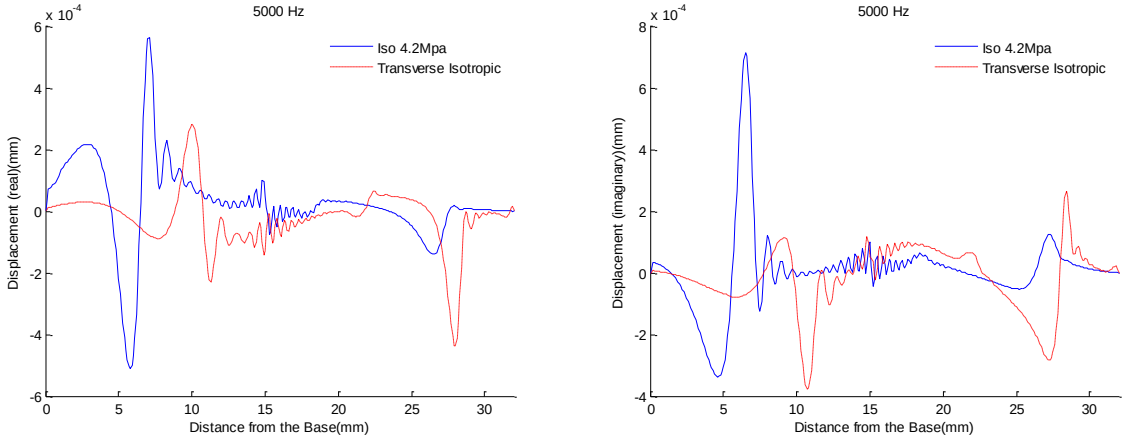


**Fig. 5. BM displacements in transverse isotropic FE model compared with those of isotropic one.**

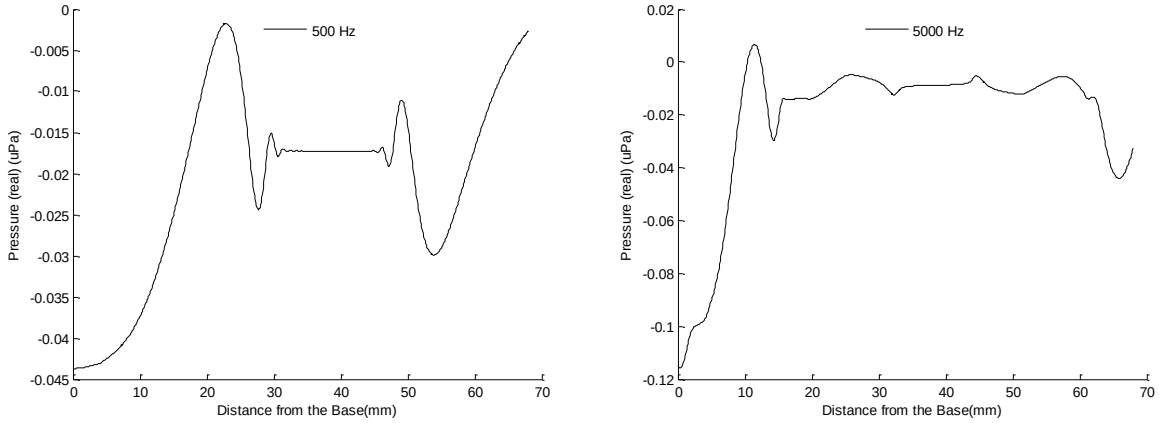


**Fig. 6. Pressure responses in the scalas with different excitation frequencies**

To compare the transverse isotropic FE model with the isotropic one, the BM displacements at 5000 Hz are plotted in Fig. 5. As expected in the cochlear map, the peak position in the isotropic FE model is closer to the base than the transverse isotropic model. We can also see in Fig. 5 that an unexpected high peak near the apex appears of which magnitude becomes larger in the transverse isotropic FE model. This peak may be related with reflected pressure wave in the scalas and be associated with noise-induced hearing loss, which is a future goal of the current research. The pressure responses along the centre line of the BM are plotted in Fig. 6 at two typical frequencies. The pressure at the scala vestibule and the scale tympani shows skew symmetric shape along the centre line because the motion of the BM reversely effects on the pressure in the scala vestibule and the scala tympani. As shown in Fig. 6, this skew-symmetry is clearer at lower frequency. However, the skew symmetry becomes unclear at higher frequency because of reflected pressure wave. The transition frequency that breaks the skew symmetry is located on near 5 kHz, which may be associated with the unexpected peak near the apex.

## 4. Conclusions

The uncoiled cochlear FE model was developed in this study. The FE model considered the transverse isotropic BM material properties and fluid-structure interactions between lymphatic fluid and the BM. The FE model predicts larger displacement than the isotropic model near the apex at 5 kHz frequency band. Moreover, the pressure responses has a transition at the same frequency band, which

may be associated with the mechanism of noise-induced hearing loss in the cochlea. This clue will be investigated as future study using transient response analysis and a coiled cochlear FE model.

## REFERENCES


1 Lee, D. and Ahn, T.-S., Statistical calibration of a finite element model for human middle ear, *Journal of Mechanical Science and Technology*, **29**(7), 2803-2815, (2015).
2 Ahn, T.-S., Baek, M.-J., and Lee, D., Experimental measurement of tympanic membrane response for finite element model validation of a human middle ear, *SpringerPlus*, **2**(1), 527, (2013).
3 Wang, X., Keefe, D.H., and Gan, R.Z., Predictions of middle-ear and passive cochlear mechanics using a finite element model of the pediatric ear, *The Journal of the Acoustical Society of America*, **139**(4), 1735-1746, (2016).
4 Zhang, X. and Gan, R.Z., Finite element modeling of energy absorbance in normal and disordered human ears, *Hearing Research*, **301**(14), 6e155, (2013).
5 Zhang, X. and Gan, R.Z., A Comprehensive Model of Human Ear for Analysis of Implantable Hearing Devices, *IEEE TRANSACTIONS ON BIOMEDICAL ENGINEERING*, **58**(10), 3025, (2011).
6 Gan, R., Reeves, B., and Wang, X., Modeling of Sound Transmission from Ear Canal to Cochlea, *Annals of Biomedical Engineering*, **35**(12), 2180-2195, (2007).
7 XU, L., et al., Finite Element Modeling of the Human Cochlea Using Fluid-Structure Interaction Method, *Journal of Mechanics in Medicine and Biology*, **15**(03), 1550039, (2015).
8 Böhnke, F. and Arnold, W., 3D-Finite Element Modelof the Human Cochlea Including Fluid-Structure Couplings, *ORL*, **61**(5), 305-310, (1999).
9 Emadi, G., Richter, C.-P., and Dallos, P., Stiffness of the Gerbil Basilar Membrane: Radial and Longitudinal Variations, *Journal of Neurophysiology*, **91**(1), 474-488, (2004).
10 Braun, K., Böhnke, F., and Stark, T., Three-dimensional representation of the human cochlea using micro-computed tomography data: Presenting an anatomical model for further numerical calculations, *Acta Oto-laryngologica*, **132**(6), 603-613, (2012).
11 NASTRAN, M., *Dynamic analysis user's guide*. MSC Software. (2010).
12 Greenwood, D.D., A cochlear frequency‐position function for several species—29 years later, *The Journal of the Acoustical Society of America*, **87**(6), 2592-2605, (1990).